

IV. DISCUSSION AND CONCLUSIONS

The calculated magnetization curve for the deformed single-crystal specimen (Fig. 1) shows the correct qualitative features. These include delayed initial penetration of the field, large hysteresis, and a shallow, broad peak just below the upper critical field. Both the calculated curve and the experimental curve are symmetric about the reversible curve, with a slight shift to lower fields for decreasing applied field. The latter is due to the internal induction lagging the applied field. Errors may occur because nonidentical specimens have been tested under nonidentical conditions.

The advantage of using detailed numerical data rather than a simple analytical fit is best seen at fields near H_{c2} , where the previous models (3-11) become inaccurate. The analysis also predicts the field at which magnetization vanishes to exceed H_{c2} very slightly, i.e., an extra "tail" on the magnetization curve. Detection of the latter was not within the sensitivity of the experiment. Larger critical current densities would be expected to give rise to larger effects, shifting the point of vanishing magnetization significantly above H_{c2} . Thus, for moderately hard or very hard super-

conductors at fields near H_{c2} , the analysis is especially useful.

The data of Fig. 2 illustrates the case where the effects of the transport currents predominate. For the solid and tubular specimens A , B , C , and D , the hysteresis increases with wall thickness because of increasing net available transport current. The initial penetration of the field is delayed beyond H_{c1} (1 kG) due to the high critical current density, which is the same in all cases. Consequently, the initial penetration of flux into the wall of the tube is the same in all cases. Specimen E in Fig. 2 demonstrates the effect of removing the most effective path for the transport current. The resulting magnetization curve is that of the bulk material which is essentially the same as that of a solid cylinder having the same cross section.

ACKNOWLEDGMENTS

The authors wish to express their appreciation for the financial support of this work by the National Science Foundation (Grant GP-2069), and helpful discussions with Professor John Wulff and Dr. K. M. Ralls.

Thermal Effects on the Fluorescence Lifetime and Spectrum of $\text{MgO}:\text{V}^{2+}$ †

B. DI BARTOLO* AND R. PECCEI‡

Laboratory for Insulation Research, Massachusetts Institute of Technology, Cambridge, Massachusetts

(Received 20 August 1964; revised manuscript received 6 November 1964)

The vibronic spectrum associated with the ${}^2E \rightarrow {}^4A_2$ transition at 8700 \AA of $\text{MgO}:\text{V}^{2+}$ has been investigated as a function of temperature. The position and the width of the purely radiative (R) line associated with this transition were measured from 4 to 460°K , and the total intensity of the fluorescence spectrum from 77 to 650°K . At low temperatures vibrational satellites are observed only on the low-energy side of the pure electronic transition, corresponding to spontaneous phonon emission; at higher temperatures they also appear on the high-energy side, corresponding to phonon absorption. With increasing temperature the vibronic bands become more intense relative to the pure electronic transition, the peaks broaden, and multiphonon processes enter and form a fluorescence continuum extending from ≈ 7000 to $10\,500 \text{ \AA}$. The fluorescence lifetime of the 2E level, which is 50 msec and nearly temperature-independent at 77°K , decreases rapidly above 200°K to ≈ 0.03 msec at 800°K . The enhancement of the transition probability of the vibronic bands, determined from the relative increase in the integrated area after correction for the temperature dependence of the absorption strength, can account for the major temperature dependence of the fluorescence lifetime, without requiring the presence of any purely nonradiative transitions.

INTRODUCTION

AN excited magnetic ion in a crystal can lose its energy by spontaneous photon, or phonon-assisted emission, or nonradiative transitions. Phonon-assisted transitions involve the emission of a photon and the

creation or annihilation of one or more phonons; they are temperature-dependent and arise from vibrational-electronic or "vibronic" interactions, wherein the vibrations may be characteristic either of the total crystal lattice or of the local environment. Radiationless transitions are also temperature-dependent; they are considered responsible for the fast relaxations from the broad absorption bands to the fluorescent level, in an ion with a $3d^3$ configuration.

The relative contributions of the vibronic and purely radiative transitions to the decay can be found directly

† Sponsored by the U. S. Air Force Office of Scientific Research, Washington, D. C., under Research Grant AF-AFOSR-62-317, and U. S. Air Force Materials Laboratory under Contract AF 33(616)8353.

* Present address: MITHRAS Inc., Cambridge, Massachusetts.

‡ Present address: Physics Department, Massachusetts Institute of Technology, Cambridge, Massachusetts.

by measuring the fluorescence intensities of the vibronic and no-phonon lines as function of temperature. The radiative lifetime of the fluorescent level can be determined from measurement or calculation of the oscillator strength of the radiative transition. Together, the two data can establish the extent of any nonradiative decay process.

$\text{MgO}:\text{V}^{2+}$ is a particularly good subject for such studies. Divalent vanadium has a $3d^3$ electronic configuration and enters the MgO lattice substitutionally at a Mg^{2+} site. The theoretical energy-level structure for the d^3 configuration in an octahedral field has been given by Tanabe and Sugano.¹ The observed fluorescence and excitation spectra for $\text{MgO}:\text{V}^{2+}$, including the low-temperature vibronic structure, has been reported by Sturge.² Since the crystalline field acting on the V^{2+} ions in MgO has cubic symmetry, any electric dipole transitions that might be allowed by the presence of a static noncentrosymmetric field are forbidden. Thus the purely electronic transition is weak and principally magnetic dipole in origin. In such a case, the vibronic transitions may make a correspondingly greater contribution to the excited-state decay. For $\text{MgO}:\text{V}^{2+}$, the integrated fluorescence intensity of the vibronic bands is indeed greater than that of the nonphonon line, even at low temperatures where the probability for vibrationally induced transitions is a minimum. Owing to the cubic symmetry, however, there are no polarized spectra to aid in identifying the character of the radiation.

EXPERIMENTAL TECHNIQUES

Preparation of the Sample

The sample used in this experiment was an MgO crystal, $1 \times 1 \times \frac{1}{2}$ cm³, with 0.025 weight % V impurity.³ Following Sturge's procedure,² the sample was heated in H_2 at 1200°C for 4 h, to favor the formation of divalent vanadium. This resulted in a large increase of the V^{2+} fluorescence and a reduction of the V^{3+} absorption which however, still overwhelmed the V^{2+} spectrum.

Apparatus

Steady-state measurements of the fluorescence spectra were made using a Jarrell-Ash 3.4-m Ebert grating monochromator (7442 grooves/in.), with a linear dispersion in the second order of ≈ 6 Å/mm. The crystal was excited with a 1-kW GE AH6 high-pressure mercury lamp. The fluorescence was observed at 90 deg from the axis of the exciting system, and was detected at the monochromator exit slit with an RCA 7102 photomultiplier tube cooled to 77°K. The spectrum was scanned and recorded using phase-sensitive detection techniques.

¹ Y. Tanabe and S. Sugano, J. Phys. Soc. Japan 9, 766 (1954).

² M. D. Sturge, Phys. Rev. 130, 639 (1963).

³ Supplied by the Norton Company, Chippawa, Ontario, Canada.

TABLE I. Fluorescence spectrum of $\text{MgO}:\text{V}^{2+}$ at room temperature.

| Line | Low-energy band | | | High-energy band | | | |
|------------|------------------------------------|------------------------------|---------------|------------------------------------|------------------------------|---------------|--------|
| | $\Delta\nu$ (cm ⁻¹) | ν (cm ⁻¹) | λ (Å) | $\Delta\nu$ (cm ⁻¹) | ν (cm ⁻¹) | λ (Å) | |
| α_r | 270 | 11 216 | 8915.8 | α_b | 260 | 11 746 | 8513.5 |
| α_r | 420 | 11 066 | 9036.7 | β_b | 410 | 11 896 | 8406.2 |
| γ_r | 490 | 10 996 | 9094.2 | γ_b | 490 | 11 976 | 8350 |
| $2\beta_r$ | 540 | 10 946 | 9135.7 | | | | |

$\Delta\nu$ is distance from R line.
 R line has wavelength: $\lambda_0 = 8706.2$ Å (11 486 cm⁻¹)

Sample temperatures between 77°K and room temperature were obtained by regulating the flow of pre-cooled N_2 gas into the inner chamber of a helium Dewar. For higher temperature measurements, the sample was placed in a quartz vessel with a nichrome wire heater. Sample temperatures were generally constant to $\approx \pm 1^\circ\text{K}$ during the 20 min required to record the total fluorescence spectrum.

The R line of $\text{MgO}:\text{V}^{2+}$ (8699 Å) was observed in the 6th order. Here the linear dispersion was 2 Å/mm.

Fluorescence lifetime measurements were made by exciting the crystal with an FX-12 EG & G flash tube. The fluorescence signal was passed through a #98 Perkin Elmer prism monochromator, detected with a 7102 cooled photomultiplier, and displayed and photographed on a Tektronix #541 oscilloscope. The time resolution of the apparatus was 5 μsec .

RESULTS

The complete spectrum of the $\text{MgO}:\text{V}^{2+}$ fluorescence emission at room temperature presents bands at both sides of the main (R) line modulated by certain characteristic frequencies (Table I). The position and width of the R line, measured from 4 to 460°K, were found to be temperature-dependent (Fig. 1). The results agree in general with those obtained by Imbusch *et al.*,⁴ but cover a wider temperature range.

The fluorescence spectrum of $\text{MgO}:\text{V}^{2+}$ was examined from 80 to $\approx 650^\circ\text{K}$. The fluorescence from 7000 to 10 500 Å associated with the ${}^2E \rightarrow {}^4A_2$ transition is shown in Fig. 2 for five different sample temperatures. The spectra illustrate the behavior of the vibrational satellites with temperature, although they are uncorrected for the decreasing response of the S-1 photomultiplier-tube cathode in the long-wavelength region.

The over-all features of the spectrum are:

- (1) Certain characteristic frequencies appear;
- (2) as the temperature goes down, the high-energy vibronic band diminishes until, at 77°K, it cannot be detected; simultaneously the peaks become increasingly sharp and shift toward smaller wavelengths;
- (3) with increasing temperature the continuum of

⁴ G. F. Imbusch, W. M. Yen, A. L. Schawlow, D. E. McCumber, and M. D. Sturge, Phys. Rev. 133, A1029 (1964).

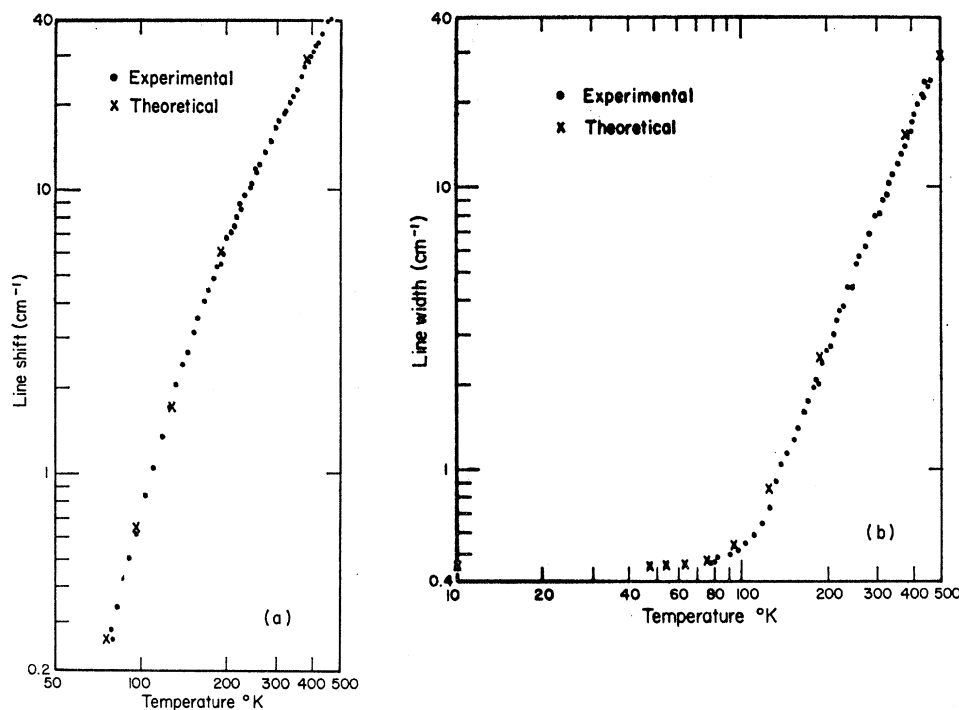


FIG. 1. (a) Thermal shift and (b) thermal broadening of the R line of $\text{MgO}:\text{V}^{2+}$. Accuracy of line position: 0.1 to 0.05 of linewidth; accuracy of width: $\pm 3\%$.

the spectrum expands more and more to wavelengths farther removed from that of the R line and grows in intensity, while the peaks tend to smooth out and disappear.

The vibronic character of the bands accompanying the sharp line fluorescence of V^{2+} in MgO was indicated by the correspondence of the fluorescence lifetime of the bands with that of the R line^{5,6} and also by the simi-

larity between the temperature shifts of the vibronic-band peaks and that of the R line.^{5,7} Furthermore, at low temperatures one would expect the disappearance of the high-energy band, since no phonons are available to be absorbed. Finally, the amplitude behavior of the side bands with temperature is characteristic of that expected for vibrational satellites.

An assignment of the peaks in the vibrational structure to various branches in the phonon spectrum has been given by Sturge² and examined in greater detail by Imbusch *et al.*⁴ The largest peaks, displaced by 270

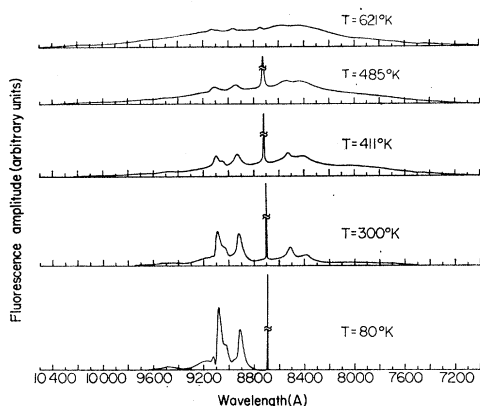


FIG. 2. Fluorescence spectrum of $\text{MgO}:\text{V}^{2+}$ at various temperatures, showing the R line at $\approx 8700 \text{ \AA}$ and the vibrational satellites. Traces uncorrected for wavelength response of the $S-1$ photomultiplier cathode.

⁵ B. Di Bartolo, Tech. Rep. 190, Lab. Ins. Res., MIT, June 1964 (unpublished).

⁶ M. J. Weber, R. R. Allen, and B. Di Bartolo (unpublished data).

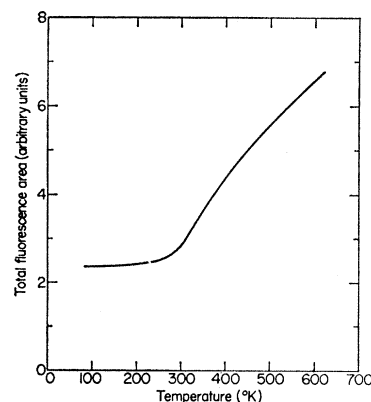


FIG. 3. Total fluorescence intensity associated with the ${}^2E \rightarrow {}^4A_2$ transition of $\text{MgO}:\text{V}^{2+}$ as function of temperature.

⁷ If the vibronic bands were really broad emission bands, a greater shift would be expected. McClure (Ref. 11), measuring the absorption spectra of Cr^{3+} in Al_2O_3 , found for the 4T_1 and 4T_2 bands shifts of $\sim 900 \text{ cm}^{-1}$ from room temperature to 700°K. The 4T_1 band of $\text{MgO}:\text{V}^{2+}$ shows a shift of $\sim 300 \text{ \AA}$ from 80° to 500°K (Ref. 6).

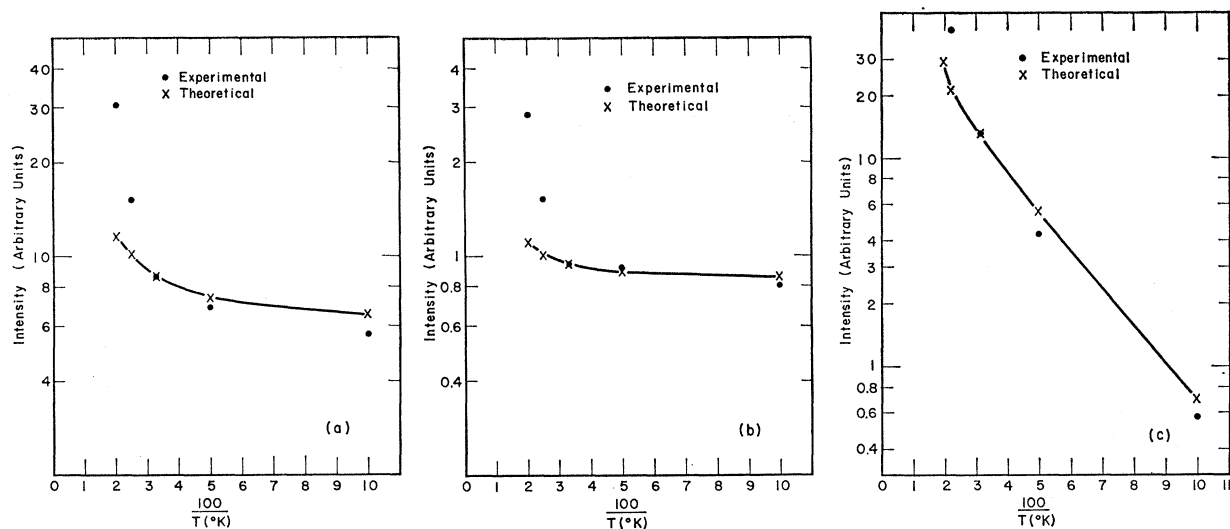


FIG. 4. Temperature dependence of intensities of $\text{MgO}:\text{V}^{2+}$ vibronic peaks. Experimental points show ratios of $I(\nu, T)$ to product of total fluorescence intensity and τ_F . (a) α_r line, (b) γ_r line, (c) α_b line.

and 490 cm^{-1} from the R line, are ascribed to acoustic and optic branches of the MgO phonon spectrum.

At high temperatures, vibrational satellites are also observed on the high-energy side of the R line, corresponding to absorption of the now present excited phonons. Owing to the different temperature dependences for phonon absorption and emission, the high- and low-energy vibronic bands are generally not expected to be identical. With increasing temperature the vibronic bands become more intense relative to the R line, line broadening occurs, and bands arising from multiphonon processes appear which combine to form the extended fluorescence continuum observed.

The integrated areas of the R line and the combined low- and high-energy vibronic bands measured at several different temperatures are given in Table II. The accuracy of the measurements was estimated to be 10%, with a 5% error due to the instability of the apparatus, and 5% to uncertainties in the corrections for photomultiplier response and grating efficiency. At high temperatures, multiphonon processes contribute to the fluorescence intensity at the position of the nonphonon line (Fig. 2); this complicated the determination of the true R -line area. The reported areas of the R line are simply those above the estimated multiphonon continuum and accordingly have a greater uncertainty at high temperatures.

The total integrated fluorescence intensity (Fig. 3) was calculated in photons/sec as a function of temperature with corrections for multiplier response, spreading in frequency of the emitted photons and grating efficiency. The temperature dependence of the most pronounced peaks of the vibronic spectrum are shown in Figs. 4(a), (b), and (c) and their intensity ratios in Figs. 5(a) and (b).

Finally, the fluorescence lifetime of the 2E level was measured from 77 to 800°K (Fig. 6).⁸

In the steady-state and pulse experiments, the exciting radiation was filtered through a CuSO_4 solution; the fluorescence was then excited mainly via the ${}^4T_1(t_2\ ^2e)$ absorption band of V^{2+} . This band is centered at $\approx 5000\text{ \AA}$ and is $\approx 1000\text{ \AA}$ wide.²

DISCUSSION AND CONCLUSIONS

Thermal Effects on the Position and Width of the R Line in $\text{MgO}:\text{V}^{2+}$

Expressions for the line shift and linewidth have been given by McCumber and Sturge⁹ in the assumption of

TABLE II. Relative fluorescence areas associated with the ${}^2E \rightarrow {}^4A_2$ transition of $\text{MgO}:\text{V}^{2+}$ as a function of sample temperature.

| Temperature ($^\circ\text{K}$) | R -line area (arbitrary units) | Total area (arbitrary units) | (Vibronics area)/(R -line area) |
|----------------------------------|----------------------------------|------------------------------|------------------------------------|
| 85 | 3.48 | 23 | 5.6 |
| 102 | 3.36 | | |
| 138 | 3.39 | | |
| 182 | 2.99 | | |
| 226 | 2.93 | | |
| 263 | 2.30 | | |
| 297 | 1.93 | 27 | 13 |
| 348 | 1.31 | 37 | 27 |
| 411 | 0.68 | 44 | 64 |
| 485 | 0.30 | 54 | 180 |
| 621 | 0.13 | 68 | 520 |

⁸ The data on fluorescence lifetime shown in Fig. 6 agree very well between 77 and 650°K with data obtained from M. J. Weber and R. R. Allen at the Research Division of Raytheon Company, on a similar sample. For a comparison of the two measurements see Ref. 5.

⁹ D. E. McCumber and M. D. Sturge, J. Appl. Phys. **34**, 1682 (1963).

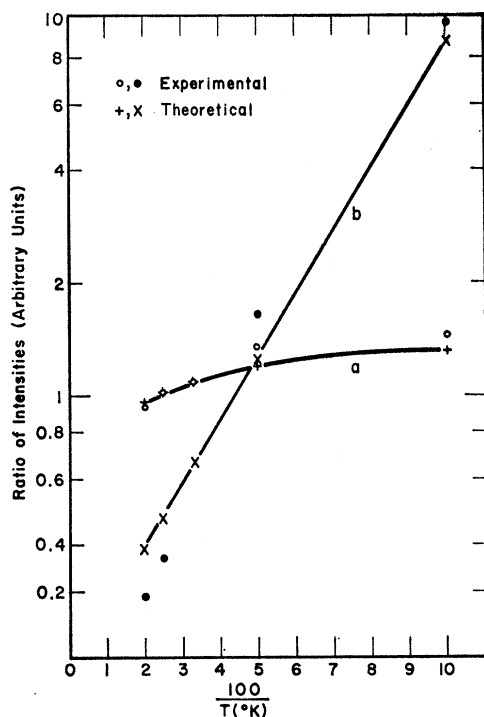


FIG. 5. Temperature dependence in $\text{MgO}:\text{V}^{2+}$ of (a) intensity ratio of γ_r to α_r line, (b) of α_r to α_b line.

a Debye spectrum of acoustic phonons:

$$\delta\lambda(T) = \alpha \left(\frac{T}{T_D} \right)^4 \int_0^{T_D/T} \frac{x^3}{e^x - 1} dx; \quad (1)$$

$$\Delta\lambda(T) = \bar{\alpha} \left(\frac{T}{T_D} \right)^7 \int_0^{T_D/T} \frac{x^6 e^x}{(e^x - 1)^2} dx, \quad (2)$$

where T_D is the Debye temperature of the crystal. We have been able to fit our experimental curve with a $T_D = 760^\circ\text{K}$, $\alpha = -400 \text{ cm}^{-1}$, $\bar{\alpha} = 377 \text{ cm}^{-1}$. In addition to $\Delta\lambda(T)$, the sample presented a "strain linewidth" of 0.45 cm^{-1} [Fig. 1(b)].

In the model from which Eqs. (1) and (2) are derived, the thermal shift of the R line is explained as due to the stationary effects of the ion-vibration interaction, and the thermal broadening as due to Raman scattering of phonons. Expression (1) represents, apart from certain constants, the total heat of the system. Although the Debye form is a poor description of the vibrational spectrum, neither the total heat nor the line shift is sensitive to fine structure in the spectrum.

In MgO , there is good agreement between the Debye temperature derived from heat-capacity measurements¹⁰ and that derived from the shift of the R lines of V^{2+} impurity. The slight disagreement between theoretical and experimental data near 100°K [Fig. 1(a)] may be

¹⁰ T. H. Barron, W. T. Berg, and J. A. Morrison, Proc. Roy. Soc. (London) **A250**, 70 (1959).

due to an increase of the Debye temperature as found from specific-heat measurements. The Debye temperature used to explain the line-shift experiments may also account for the linewidth dependence on temperature.

At high temperature the line is Lorentzian, as expected for Raman broadening; at 4°K it appears close to a Gaussian (Fig. 7). The latter is expected from a random distribution of strains which affect the local crystal field and hence the ionic energy levels.

The Fluorescence Lifetime and the Vibronic Spectrum of $\text{MgO}:\text{V}^{2+}$

In the steady-state experiments, the excitation of an ion to the 4T_1 level is followed by a rapid decay to the 2E (fluorescent) level. We have essentially a three-level system. When the rate of induced transitions is slow compared to the decay rate, the equilibrium number of ions in the fluorescent level is given by

$$N_2 \approx N \langle \sigma I_{ss} \rangle \tau_F, \quad (3)$$

where N is the total number of ions in the crystal, σ the absorption cross section, I_{ss} the steady-state intensity of the exciting radiation in the crystal, and τ_F the total decay time of the fluorescent level. The angle brackets denote an integral over the spectral distribution of I_{ss} .

A fluorescent signal $I(\nu, T)$ is given by

$$I(\nu, T) = N_2 W^r(\nu, T) = N \langle \sigma(T) I_{ss} \rangle \tau_F(T) W^r(\nu, T) [\text{photons/sec}]. \quad (4)$$

The radiative probability W^r is considered to include

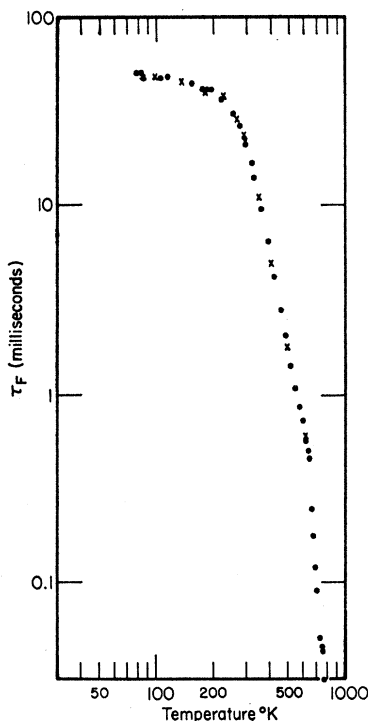


FIG. 6. Temperature dependence of the fluorescence lifetime of the 2E state of $\text{MgO}:\text{V}^{2+}$. Accuracy of individual points $\approx 5\%$. ● = fluorescence lifetime; x = ratio of R -line intensity to total fluorescence intensity.

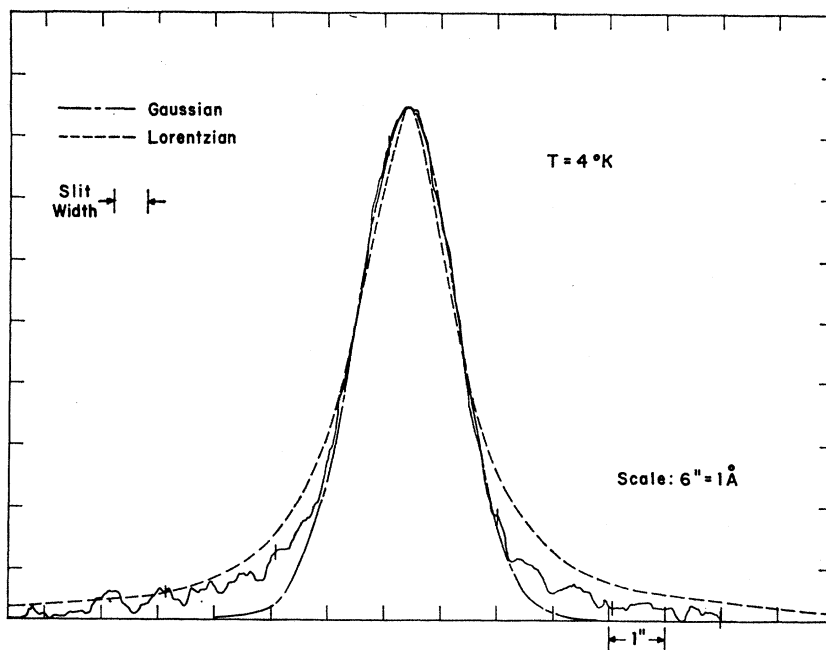
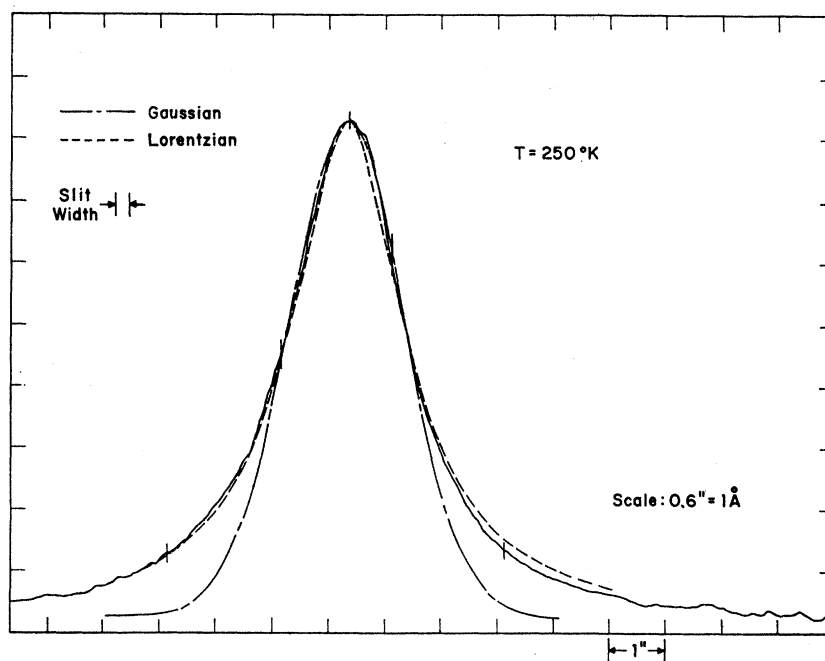


FIG. 7. Line shape of R line of $\text{MgO}:\text{V}^{2+}$ at 4 and 250°K.



both nonphonon and phonon-assisted transitions. The former is in general temperature-dependent; hence the temperature dependence of W^r . Similarly, the absorption cross section σ may be enhanced by temperature-dependent vibrational interactions.

The behavior of the total fluorescence (Fig. 3) was measured by integrating the fluorescence signal $I(\nu, T)$ in Eq. (4) over all frequencies ν . The observed increase in total intensity reflects the increase in the absorption

cross section with temperature and its dominance over any nonradiative transitions. Similar increases in absorption cross section of transition metal ions with temperature have been reported^{11,12} by direct observation of the absorption spectra. For the fluorescence of V^{2+} in MgO , the magnitude and temperature depend-

¹¹ D. S. McClure, J. Chem. Phys. 36, 2657 (1962).

¹² D. G. Holmes and D. S. McClure, J. Chem. Phys. 26, 1686 (1957).

ence of $\sigma(T)$ in Eq. (4) include any modifications due to the presence of V^{3+} or other impurities in the crystal used. The fluorescence lifetime is a measure of the combined probabilities for purely radiative W^r (R line), vibronic W^r (Vib) and nonradiative W^{nr} decays. Their relative importance for the fluorescence decay can be determined from measurements of the temperature dependence of τ_F , σ , and the fluorescence intensities, coupled with the oscillator strength of the R line. Although the magnitude and temperature dependence of τ_F can be measured directly, this could not be done for σ in our sample of $MgO:V^{2+}$ because of its relative weakness and the masking effects of other impurity absorptions.

However, while the fluorescence signals are proportional to the product of σ , τ_F , and W^r , the temperature dependence of the total radiative probability W^r (R line) + $W^r(vib)$ can be determined from the ratio of the total fluorescence intensity to that of the R line, assuming $W^r(R)$ independent of temperature. The inverse of this ratio (Table II) is shown in comparison with τ_F (Fig. 6), normalized to τ_F in the low-temperature limit where τ_F is approximately constant. Between 80 and 620°K, the T dependence of τ_F and that of the inverse of the total radiative probability agree very well. Consequently, we may say that if nonradiative processes contribute to the shortening of the fluorescence lifetime, they must have the same temperature dependence as the total radiative probability.

A consequence of this fact is that the agreement obtained in Fig. 6 allows us to take the total fluorescence intensity as a measure of the pumping probability $\langle\sigma I_{ss}\rangle$. With this, and using the measured values of τ_F , the temperature dependences of the 270- and 490-cm⁻¹ vibronic peaks were derived. The T dependence of a vibronic transition involving a single phonon of frequency ν is governed by the Bose-Einstein factors $e^x(e^x-1)^{-1}$ and $(e^x-1)^{-1}$ for emission and absorption, respectively, where $x=h\nu/kT$. This general behavior was observed for the 270-cm⁻¹ (α)¹³ and 490-cm⁻¹ (γ)¹³ peaks although at high temperatures some disagreement from the one-phonon temperature dependence was noticed, due probably to the superimposed contribution from multiphonon vibronic transitions (Fig. 4). General agreement with the expected temperature dependences was also found for the ratios of the intensities of the γ_r to α_r and of α_r to α_b lines (Fig. 5).

If an ion in an excited state decays only by radiative or vibronic processes, the radiative lifetime τ_0 is related to the fluorescence lifetime by

$$\tau_0 = \tau_F(T)[S(T)+1], \quad (5)$$

¹³ For this notation see Table I.

where $S(T)$ is the ratio of the vibronic area to the R -line area. By taking the values of S and τ_F at any temperature from Table II, we find for τ_0 a value of ≈ 0.32 sec. τ_0 can also be derived from the knowledge of the oscillator strength of the radiative transition. Sturge² attempted to measure the absorption coefficient of the ${}^4A_2 \rightarrow {}^2E$ transition but could only set an upper limit on the oscillator strength of 2×10^{-9} . We also tried to measure the absorption in our sample, but without success. Recent calculations⁶ found for τ_0 a value of 0.39 sec, which agrees quite well with the experimental value derived in the assumption that radiationless processes are ineffective in depleting the 2E state.

The above results indicate that the magnitude and T dependence of the fluorescence lifetime below 650°K can be accounted for by the enhanced probability for phonon-assisted transitions without requiring the presence of any nonradiative processes. This is perhaps not too surprising, for if one attempts to invoke multiphonon nonradiative processes, more than twenty phonons would be required to conserve the energy of the electronic transition. The T dependence for such a process is expected to be more pronounced than that observed for τ_F between 80 and 650°K.

Similar results are expected to be found in systems like Cr^{3+} in MgO and Al_2O_3 . The vibronic spectrum of ruby has been observed by Burns and Nathan,¹⁴ but no careful study of the vibronic bands as dependent on temperature has been done as yet. The presence of an axis in the crystal enables an investigation on the explicit nature of the vibronic emission in ruby. Moreover, the temperature dependence of the absorption band areas is already known.¹¹

Rare-earth-doped crystals are less suitable for study, because the closeness of the levels of the ground-state multiplet can make pure radiative lines close to vibronic satellites, and thus generate difficulties in the interpretation of the spectrum. However, gadolinium, which has an S ground state, would certainly be suitable for a complete study to relate the vibronic emission to the lifetime of the fluorescent level.

ACKNOWLEDGMENTS

The authors wish to thank Professor Perry A. Miles for his assistance and advice during the preparation of this work. Thanks are also due to Professor George Koster, to Dr. Marvin Weber, and to the Research Division of Raytheon Company for helpful discussions, and also to the members of the Laboratory for Insulation Research, Massachusetts Institute of Technology, for their continuous help.

¹⁴ G. Burns and M. I. Nathan, J. Appl. Phys. **34**, 203 (1963).